















ORIGINAL RESEARCH

# Stent Optimization Using Optical Coherence Tomography and Its Prognostic Implications After Percutaneous Coronary Intervention

Himanshu Rai , MSc, PhD; Fiona Harzer ; Tatsuhiko Otsuka , MD; Youssef S. Abdelwahed , MD; Paula Antuña, MD; Florian Blachutzik, MD; Tobias Koppa, MD; Lorenz Räber , MD; David M. Leistner , MD; Fernando Alfonso , MD; Holger Nef, MD; Masaru Seguchi, MD; Alp Aytakin, MD; Erion Xhepa , MD, PhD; Sebastian Kufner , MD; Salvatore Cassese , MD, PhD; Karl-Ludwig Laugwitz , MD; Robert A. Byrne , MB, BCh, PhD; Adnan Kastrati , MD; Michael Joner , MD

**BACKGROUND:** Stent underexpansion has been known to be associated with worse outcomes. We sought to define optical coherence tomography assessed optimal stent expansion index (SEI), which associates with lower incidence of follow-up major adverse cardiac events (MACEs).

**METHODS AND RESULTS:** A total of 315 patients (involving 370 lesions) who underwent optical coherence tomography-aided coronary stenting were retrospectively included. SEI was calculated separately for equal halves of each stented segment using minimum stent area/mean reference lumen area ( $[(\text{proximal reference area} + \text{distal reference area})/2]$ ). The smaller of the 2 was considered to be the SEI of that case. Follow-up MACE was defined as a composite of all-cause death, myocardial infarction, stent thrombosis, and target lesion revascularization. Average minimum stent area was 6.02 (interquartile range, 4.65–7.92) mm<sup>2</sup>, while SEI was 0.79 (interquartile range, 0.71–0.86). Forty-seven (12.7%) incidences of MACE were recorded for 370 included lesions during a median follow-up duration of 557 (interquartile range, 323–1103) days. Receiver operating characteristic curve analysis identified 0.85 as the best SEI cutoff ( $<0.85$ ) to predict follow-up MACE (area under the curve, 0.60; sensitivity, 0.85; specificity, 0.34). MACE was observed in 40 of 260 (15.4%) lesions with SEI  $<0.85$  and in 7 of 110 (6.4%) lesions with SEI  $\geq 0.85$  ( $P=0.02$ ). Least absolute shrinkage and selection operator regression identified SEI  $<0.85$  (odds ratio, 3.55; 95% CI, 1.40–9.05;  $P<0.01$ ) and coronary calcification (odds ratio, 2.47; 95% CI, 1.00–6.10;  $P=0.05$ ) as independent predictors of follow-up MACE.

**CONCLUSIONS:** The present study identified SEI  $<0.85$ , associated with increased incidence of MACE, as the optimal cutoff in daily practice. Along with suboptimal SEI ( $<0.85$ ), coronary calcification was also found to be a significant predictor of follow-up MACE.

**Key Words:** major adverse cardiac events ■ optical coherence tomography ■ percutaneous coronary intervention ■ stent expansion index

Optical coherence tomography (OCT) is a potent intravascular imaging modality that provides high-resolution (10–20  $\mu\text{m}$ ) cross-sectional images of coronary arteries and can be used for guiding percutaneous coronary interventions (PCIs). In the DOCTORS (Does Optical Coherence Tomography

Optimize Results of Stenting) trial,<sup>1</sup> OCT guidance during PCI resulted in a statistically significant improvement in postprocedural fractional flow reserve compared with angiography-guided PCI in a non-ST-segment-elevation acute coronary syndrome cohort. This effect was mainly driven by improved stent

Correspondence to: Michael Joner, MD, Deutsches Herzzentrum München, Technische Universität München, Lazarettstrasse 36, 80636 Munich, Germany. Email: michaeljoner@me.com

Supplemental Material for this article is available at <https://www.ahajournals.org/doi/suppl/10.1161/JAHA.121.023493>

For Sources of Funding and Disclosures, see page 11.

© 2022 The Authors. Published on behalf of the American Heart Association, Inc., by Wiley. This is an open access article under the terms of the Creative Commons Attribution-NonCommercial-NoDerivs License, which permits use and distribution in any medium, provided the original work is properly cited, the use is non-commercial and no modifications or adaptations are made.

JAHA is available at: [www.ahajournals.org/journal/jaha](http://www.ahajournals.org/journal/jaha)

## CLINICAL PERSPECTIVE

### What Is New?

- In a retrospective, unselected, real-world sample of 370 lesions, we defined an optical coherence tomography–assessed optimal stent expansion index cutoff of 0.85, which is associated with lower incidence of subsequent major adverse cardiac events, where stent expansion index <0.85 and coronary calcification were identified as independent predictors of follow-up major adverse cardiac event.

### What Are the Clinical Implications?

- Our results indicate that a relative metric of stent expansion index  $\geq 0.85$  could potentially be a superior indicator of optimal stent expansion, as opposed to previously established absolute metrics of minimum stent/lumen areas, especially for diverse real-world populations.

## Nonstandard Abbreviations and Acronyms

<b>MACE</b>	major adverse cardiac events
<b>MSA</b>	minimum stent area
<b>SEI</b>	stent expansion index

expansion in the OCT-guided group. Subsequently published ILUMIEN III (OPTIMIZE PCI: Multicenter Randomized Trial of OCT Compared to IVUS and Angiography to Guide Coronary Stent Implantation) trial,<sup>2</sup> which was much more liberal in terms of inclusion of varied presentation diagnoses, suggested that OCT-guided PCI resulted in noninferior minimum stent area (MSA) as compared with intravascular ultrasound–guided PCI. The largest published network meta-analysis to date also suggested that intravascular ultrasound or OCT-guidance during PCI was associated with significant reductions in major adverse cardiac events (MACEs) and cardiovascular mortality during follow-up as opposed to angiographic guidance.<sup>3</sup> Achieving optimal stent expansion during PCI seems to be one of the key factors in reducing future events; however, significant ambiguity exists when it comes to the exact definition of optimal stent expansion during PCI. While OCT imaging was proven superior to other intravascular imaging modalities in delineating stent expansion, there is ongoing debate to define an optimal cutoff in terms of stent expansion index (SEI) demonstrating reduced event recurrence after PCI.<sup>1,2,4</sup> Also, there is lack of insight into SEI obtained in OCT-guided PCIs in day-to-day

practice and its association with future cardiovascular events. Against this background we aimed to collect clinical cases undergoing OCT-guided stent implantation, where final PCI results were captured by OCT imaging to derive insights into SEI achieved in daily practice and to derive a cutoff for SEI, which is clinically associated with lower incidence of MACEs during follow-up.

## METHODS

The data that support the findings of this study are available from the corresponding author upon reasonable request.

### Study Design

The present project represents an investigator-initiated, retrospective observational effort in which 5 high-volume centers of central Europe pooled their cases for analysis at a centralized core lab located at ISAResearch Center, Deutsches Herzzentrum München, Technische Universität München, Munich, Germany.

### Ethics

Local ethical approval was granted at Charité-University Medicine Berlin (EA4/021/15), and Inselspital Bern (NCT02241291). Ethical approval and patient consent were waived in all centers but Charité-University Medicine Berlin and Inselspital Bern since all procedures including OCT imaging were clinically indicated and data processing was completely anonymized.

### Study Population

During the period between 2012 and 2018, operators at our 5 study centers performed post-PCI OCT imaging in a total of 612 treated lesions. Reasons to use OCT in these cases and the criteria used for OCT guidance and final optimization were those of local investigators during routine clinical practice. OCT runs after index PCI and relevant baseline clinical data of all these cases were transferred to our centralized core lab for further assessment. After arrival of anonymized data from participating centers, further screening was carried out to identify noneligible and unanalyzable cases. Eligibility criteria for our present study were as follows: (1) patients  $\geq 18$  years of age, (2) final procedural result captured with OCT imaging, and (3) angiographic films of the index procedure, along with critical baseline clinical data available for analysis.

After initial quality check, 242 OCTs of treated lesions were excluded from the study for the following reasons: (1) post-PCI OCT capturing final result not available ( $n=194$ ); (2) lacking angiographic evidence of

final result capture using OCT (n=21); (3) OCT unanalyzable because of blood/rotational artifacts (n=14); (4) OCT captured only <50% of the implanted length (n=4); and (5) unavailability of critical clinical data (n=9). This left a total of 370 imaged lesions (315 cases), which were included in the present study. The study flow is depicted in Figure 1. American College of Cardiology/American Heart Association criteria were used for angiographic/lesion characterization,<sup>5</sup> whereas Mintz criteria was used to grade coronary calcification.<sup>6</sup> Clinical follow-up data for these cases was then requested from all study centers, which was blinded from OCT analysts.

## OCT Image Acquisition and Core Lab Analysis

OCT image acquisition was performed with the ILUMIEN OPTIS system and Dragonfly OPTIS imaging catheter (Abbott Vascular, Santa Clara, CA). Unitary acquisition length was 75 or 54 mm, axial scanning rate was 100 Hz, and the rate of pullback acquisition was 36 mm or 18 mm/sec.

Offline OCT analysis was performed using Windows-based QIvus 3.0.30.0 software (Medis Medical Imaging Systems, Leiden, the Netherlands) by experienced analysts. Contiguous cross-sections (spaced 1 mm apart) within the stented and reference segments were analyzed. Software-aided automatic lumen contour detection was performed throughout the stented segment and both reference segments (5 mm of distal and proximal stent edge), delineating lumen area in each analyzed frame. Software-enabled automatic strut detection was followed by manual corrections in case of anomalies. These strut points were later connected to delineate stent contour. Circumferential area limited by the stent contour was identified as stent area of that analyzed frame. SEI assessment was performed using the split

technique explained in Figure 2, which essentially is a modified ILUMIEN III trial methodology.<sup>2</sup> First, the stented segment was split into 2 equal halves in the longitudinal-vessel view. Stented segments, which had a major side branch of  $\geq 2.5$  mm, were split from the midpoint of the bifurcation. SEI was then calculated independently for both distal and proximal halves using the formula  $SEI = MSA / ([\text{proximal reference area} + \text{distal reference area}] / 2)$ . The smallest SEI among the 2 prevailed as the SEI of that case. Reference lumen area was defined as a representative (preferably disease-free/minimal disease) area contained within the reference segment (5 mm proximal and distal to the stented segment and 5 mm upstream and downstream from the split frame). If the pullback lacked analyzable reference segments, reference areas were taken from the stented segment itself. The process employed for reference frame selection is explained in detail in Data S1 and displayed as Figure S1. For long lesions, where the stented segment was contained in  $\geq 2$  pullbacks, anatomic landmarks such as side branches were used as bookmarks for splitting the analysis. About 5% of lesions (n=20) were randomly selected to be re-analyzed by the primary and 1 secondary assessor to ascertain inter- and intrarater reliability.

Qualitative OCT characteristics of every included case were also assessed. Intrastent thrombus was defined as a  $\geq 0.2$ -mm mass protruding from the luminal edge of a stent strut or floating within the lumen visible in the post-PCI OCT. Intrastent plaque protrusion was defined as any intraluminal mass protruding at least 0.2 mm within the luminal edge of a stent strut, further classified as (1) major: protrusion area at the tissue protrusion site is  $\geq 10\%$  of the stent area; or (2) minor: protrusion area at the tissue protrusion site  $< 10\%$  of the stent area. Untreated reference segment disease was defined as a minimum lumen area in the reference segment (5 mm upstream and downstream from the stent edges)  $\leq 50\%$  of the nearest stent area, and subclassified as low ( $\leq 90^\circ$  of lipid arc), medium ( $> 90^\circ$  to  $< 180^\circ$  of lipid arc), and high ( $\geq 180^\circ$  of lipid arc) lipid arc. Post-PCI edge dissections were defined as visible edge dissection  $> 60$  degrees of the circumference of the vessel or  $> 3$  mm in length (major) or any visible dissection  $< 60^\circ$  of the circumference of the vessel or  $< 3$  mm in length (minor). Incompletely apposed stent struts separated by the adjacent lumen contour with a distance of  $\geq 0.2$  mm, while not associated with any side branch or present in the MSA frame leading to suboptimal stent expansion, were considered as a minor malapposition. Malappositions were considered major when they appeared in the MSA frame and led to suboptimal stent expansion.

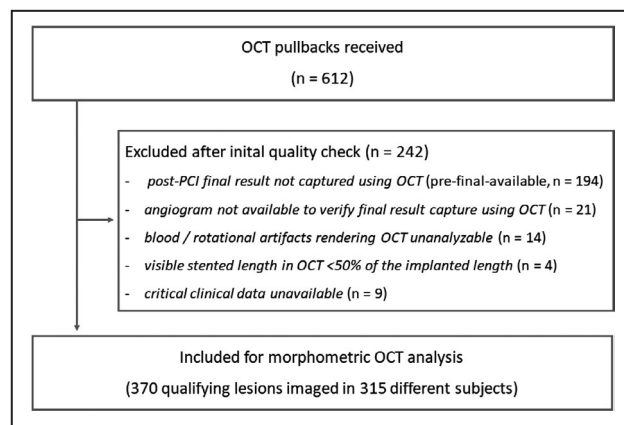


**Figure 1. Study flowchart.**  
OCT indicates optical coherence tomography.

## End Points

MACE, which was a composite of all-cause death, myocardial infarction (MI), stent thrombosis, and target

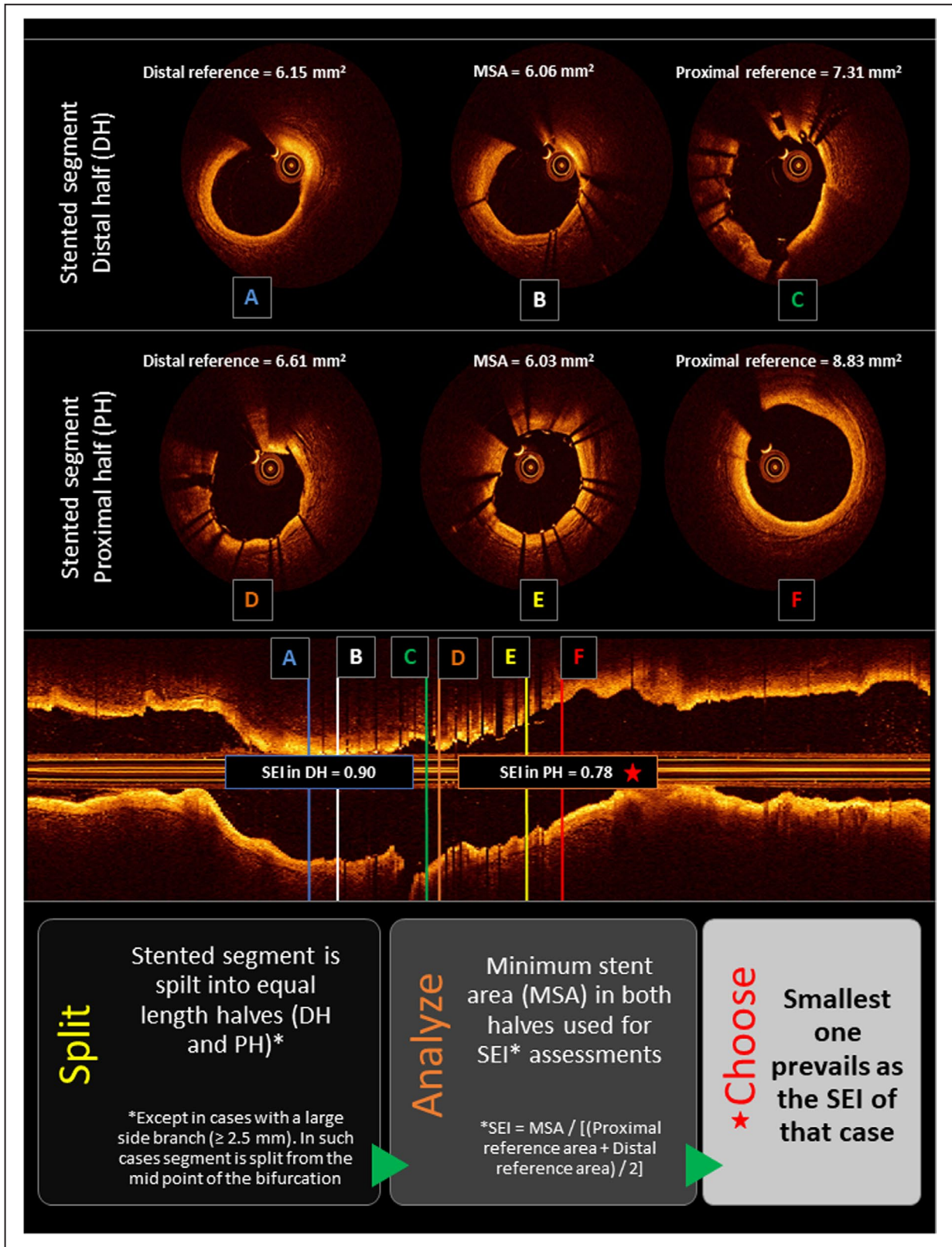


**Figure 2.** Stent expansion index assessment methodology. MSA indicates minimum stent area; and SEI, stent expansion index.

lesion revascularization during post-PCI follow-up was the primary end point of the present study. Events were adjudicated at respective study centers by site investigators using standard definitions. All-cause death included death occurring from any cause. MI was defined as rise and/or fall of cardiac troponin with at least 1 value above the 99th percentile of the upper reference limit and any 1 of the following: (1) ischemic symptoms, (2) new or presumed new significant ST-segment–T wave changes or new left bundle branch block; (2) development of pathological Q waves in the ECG; (3) imaging evidence of new loss of viable myocardium or new regional wall motion abnormality; or (4) identification of an intracoronary thrombus by angiography or autopsy.<sup>7</sup> Incidence of periprocedural MI, however, was systematically assessed only at 1 of our 6 participating centers. Stent thrombosis was defined according to Academic Research Consortium's criteria<sup>8</sup> but not further classified into definite, probable, and possible. Target lesion revascularization was defined as any repeat PCI of the target lesion (stented segment+5-mm proximal and distal edge) or bypass surgery of the target vessel performed for restenosis or other complication of the target lesion but not further classified into clinically indicated/not clinically indicated.<sup>9</sup>

### Statistical Analysis

Statistical analysis was performed using JMP version 13.1 (SAS Institute, Cary, NC) and R version 3.5.0 (R Foundation for Statistical Computing, Vienna, Austria) software. Data are presented as counts (%), mean±SD, or median with interquartile range (IQR). Differences between groups were assessed using the chi-square (or Fisher's exact test when the expected cell value was <5). Continuous data were compared using the Student *t*-test or Mann-Whitney *U* test, depending on the distribution of the analyzed variable. A 2-sided *P* value of <0.05 was considered statistically significant. Receiver operating characteristic curve analysis was performed, and Youden's (J) index was used to ascertain SEI cutoff capable of predicting MACE during follow-up. Optimal cutoff was rounded up including 2 decimals. The cohort was dichotomized into subgroups using the obtained SEI cutoff. Selection of covariates in the multivariate generalized regression model was performed using the least absolute shrinkage and selection operator regression method after entering all available candidates, which included age; sex; body mass index; diabetes; hypertension; family history of coronary artery disease (CAD); smoking status; dyslipidemia; prior MI; prior PCI; prior coronary artery bypass surgery; left ventricular ejection fraction; presence of single, double, or triple vessel disease; presence of ≤2 or 3-vessel disease; number of treated vessels (1, 2,

or 3); restenosis; lesion complexity (B2/C); bifurcation lesions; moderate/severe coronary calcification; stent overlap; postdilation status; coronary dissection; untreated reference segment disease; MSA <4.5 mm<sup>2</sup>; distal reference lumen area <4.5 mm<sup>2</sup>; proximal reference lumen area <4.5 mm<sup>2</sup>; middle reference lumen area <4.5 mm<sup>2</sup>; and optimal/suboptimal SEI. Survival analysis was performed according to the Kaplan-Meier method using the log-rank test to assess differences in cumulative survival rates as time to first event among dichotomized lesion cohorts. In addition, marginal Cox proportional hazard models were used to address the clustered nature of lesion-level time-to-first-event analysis (370 lesions in 315 patients). Inter- and intrarater reliability of OCT-based SEI was assessed using the interclass correlation coefficient in ~5% of randomly selected cases. Interclass correlation coefficient >0.7 was taken to indicate a strong correlation. Here also, a 2-sided *P* value <0.05 was deemed to be statistically significant.

### RESULTS

The mean age of our 315-case cohort (370 lesions) was 64.6±11.7 years. Of them, 78.7% were men, 22.9% had diabetes, 75.9% had hypertension, 54.0% were ever-smokers, and 34.9% had a positive family history of CAD. Most of the patients had a stable CAD diagnosis at presentation during the index PCI (40.0% arrived with stable angina and 21.9% with an asymptomatic CAD-angina equivalent). On the other hand, 11.4% cases had ST-segment–elevation MI, and 21.3% had non–ST-segment–elevation MI, while 5.4% had unstable angina at presentation. A total of 30.3% of cases had a history of prior MI, while 37.8% and 9.8% had prior PCI and coronary artery bypass surgery, respectively. Baseline characteristics of the case cohort are summarized in Table 1.

Angiographic/lesion characteristics of our studied cohort are summarized in Table 2. Almost half of the included lesions (48.9%) were located in the left anterior descending artery. A total of 9.5% of the included lesions were restenotic, 20.3% had a major bifurcation, and 30.5% had moderate to severe calcification. In total, 57.6% of treated lesions were complex in nature (type B2/C). The majority of lesions had pre-PCI TIMI 3 (Thrombolysis in Myocardial Infarction) flow (84.3%), and 90% of the included lesions were covered with a single stent/scaffold. The mean number of stents/scaffolds implanted per lesion was 1.11±0.34. A total of 81.6% of lesions were stented with conventional, metallic generation-2 drug-eluting stents, while 17.6% were stented with bioresorbable vascular/resorbable magnesium scaffolds during the index PCI. A total of 231 (73.3%) patients received 1 stent each, 73 (23.2%) patients received 2 stents each, 9 (2.9%) patients

**Table 1. Baseline Characteristics**

Baseline characteristics	n (%)
Cases	315
Age, y	64.6±11.7
Body mass index, kg/m <sup>2</sup> *	27.5±4.6
Male sex	248 (78.7)
Diabetes	72 (22.9)
Hypertension	239 (75.9)
Family history of coronary artery disease	110 (34.9)
Ever smoker <sup>†</sup>	168 (54.0)
Dyslipidemia	204 (64.8)
Clinical presentation	
ST-segment–elevation myocardial infarction	36 (11.4)
Non–ST-segment–elevation myocardial infarction	67 (21.3)
Unstable angina	17 (5.4)
Stable angina	126 (40.0)
Asymptomatic coronary artery disease	69 (21.9)
Prior myocardial infarction <sup>‡</sup>	95 (30.3)
Prior percutaneous coronary intervention	119 (37.8)
Prior coronary artery bypass surgery	31 (9.8)

Data shown as mean±SD or number (percentage).

\*Data available for 76.8% of study sample (242 cases).

<sup>†</sup>Data available for 98.7% of the study sample (311 cases).

<sup>‡</sup>Data available for 99.7% of the study sample (314 cases).

received 3 stents each, and 2 (0.6%) patients received 4 stents each, which was a combined total of 412 stents in 315 patients (data not shown). Distribution at lesion level was as follows: 333 (90%) lesions received 1 stent each, 35 (9.5%) lesions 2 stents each, while 3 (0.8%) lesions received 3 stents each, which was a combined total of 412 stents in 370 lesions. The maximum stent/scaffold diameter used was 3 (IQR, 2.75–3.50) mm, while total stented length was 21 (IQR, 15–28) mm. Stent overlap was observed in 34.9% of lesions and 56.2% of lesions received post-dilation. TIMI 3 flow was achieved in all included lesions at the end of the index procedure. Medications prescribed at discharge after index PCI are summarized in Table S1 in Data S1. A total of 94.6% received aspirin, while 100% received ADP receptor antagonists.

Clinical follow-up was available at a median of 557 (IQR, 323–1103) days during which we recorded 47 (12.7%) MACE events (among 13.7% [43/315 cases]). Among MACE components, all-cause death was the most common (n=26), followed by MI, target lesion revascularization, and stent thrombosis (n=20, 14, and 5, respectively). A total of 18 events were overlapping and therefore counted once for our cumulative outcome of MACE. Events during follow-up are summarized in Table 3.

Receiver operating characteristic curve analysis along with Youden's (J) index was applied, which ascertained an SEI cutoff of <0.85, which could predict

**Table 2. Lesion/Angiographic Characteristics**

Procedural characteristics	n (%)
Lesions	370
Lesion location	
Left main stem	10 (2.7)
Left anterior descending	181 (48.9)
Left circumflex	51 (13.8)
Right coronary	102 (27.6)
Small side branches	26 (7.0)
Restenotic lesions	35 (9.5)
Complex lesions (B2/C)	213 (57.6)
Bifurcation	75 (20.3)
Calcification	113 (30.5)
TIMI flow (pre-intervention)	
0	29 (7.8)
1	5 (1.4)
2	24 (6.5)
3	312 (84.3)
Number of stents/scaffolds implanted	
1	333 (90)
2	35 (9.5)
3	3 (0.8)
Mean number of stents/scaffolds implanted	1.11±0.34
Stent/scaffold type*	
Metallic generation-2 drug eluting stent	301 (81.6)
Bioresorbable vascular scaffold/resorbable magnesium scaffold	65 (17.6)
Bare metal stent	3 (0.8)
Maximum stent/scaffold diameter, mm*	3.0 (2.75, 3.50)
Total stented/scaffolded length, mm*	21 (15, 28)
Stent overlap <sup>†</sup>	103 (34.9)
Post-dilation	208 (56.2)
TIMI flow (post-intervention) <sup>‡</sup>	
0	0 (0)
1	0 (0)
2	0 (0)
3	365 (100)
Glycoprotein IIb/IIIa use <sup>‡</sup>	18 (4.9)

Data shown as number (percentage), mean±SD or median (interquartile range). TIMI indicates Thrombolysis in Myocardial Infarction.

\*Data available for 99.7% of study sample (369 lesions).

<sup>†</sup>Data available for 79.7% of study sample (295 lesions).

<sup>‡</sup>Data available for 98.6% of study sample (365 lesions).

MACE during post-PCI follow-up (Figure 3). Receiver operating characteristic curve analysis returned with an area under the curve of 0.60, sensitivity of 0.85, and specificity of 0.34. Included lesions were then dichotomized into groups with optimal SEI (≥0.85, n=110) and suboptimal SEI (<0.85, n=260). The Kaplan-Meier curve for MACE-free survival was then generated among the dichotomized cohort, which showed modest separation

**Table 3. Events During Follow-Up**

	Whole cohort (370 lesions from 315 patients)	Optimal SEI (110 lesions from 105 patients)	Suboptimal SEI (260 lesions from 210 patients)
Follow-up duration, d	557 (323–1103)	502 (255–1011)	598 (351–1179)
All-cause death	26 (7.0)	3 (2.7)	23 (8.8)
Myocardial infarction	20 (5.4)	5 (4.5)	15 (5.8)
Stent thrombosis	5 (1.4)	1 (0.9)	4 (1.5)
Target lesion revascularization	14 (3.8)	1 (0.9)	13 (5.0)
Stroke	9 (2.4)	2 (1.8)	7 (2.7)
Major adverse cardiac events (MACE)*	47 (12.7)	7 (6.4)	40 (15.4)

Data shown as median (interquartile range) or number (crude percentages). Optimal stent expansion index (SEI) is defined as SEI ≥0.85, whereas suboptimal SEI is defined as SEI <0.85.

\*MACE is defined here as a composite of all-cause death, myocardial infarction, stent thrombosis and target lesion revascularization during follow-up.

between the subgroups, but the difference did not reach statistical significance ( $P=0.064$ ) (Figure 4). A marginal Cox regression model to account for the clustered nature of lesion-level analysis confirmed this trend without reaching statistical significance ( $P=0.16$ ).

Results obtained after qualitative assessment and morphometric analysis for all included OCTs are summarized in Tables 4 and 5, respectively, and discussed in detail in Data S1.

Generalized regression analysis identified triple-vessel disease ( $P=0.025$ ), angiographically assessed

moderate/severe coronary calcification at baseline ( $P=0.033$ ), and SEI <0.85 ( $P=0.006$ ) as predictors of follow-up MACE. However, subsequently performed adaptive least absolute shrinkage and selection operator regression rendered only SEI <0.85 (odds ratio, 3.55; 95% CI, 1.40–9.05;  $P=0.008$ ) and coronary calcification (odds ratio, 2.47; 95% CI, 1.00–6.10;  $P=0.05$ ) as independent predictors of MACE during follow-up (Figure 5). A further sensitivity analysis was performed only in the cohort treated with generation-2 metallic stents ( $n=305$  lesions), the

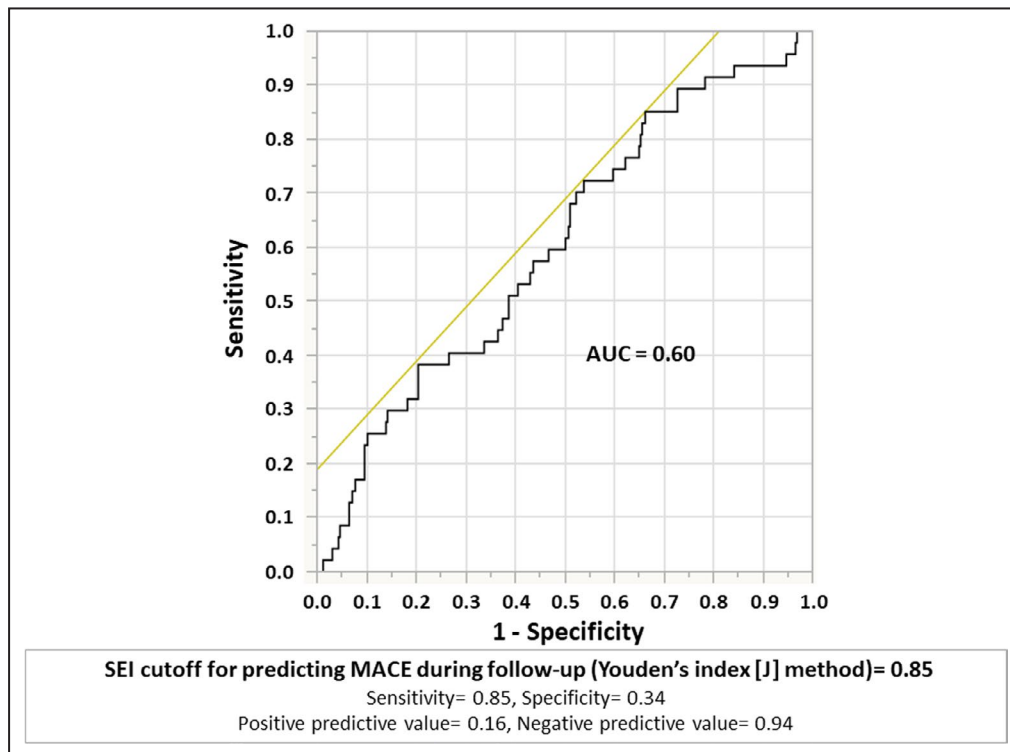


**Figure 3. ROC curve analysis producing SEI cutoff to predict MACE at follow-up.** AUC indicates area under the curve; MACE, major adverse cardiac events; ROC, receiver operating characteristic; and SEI, stent expansion index.

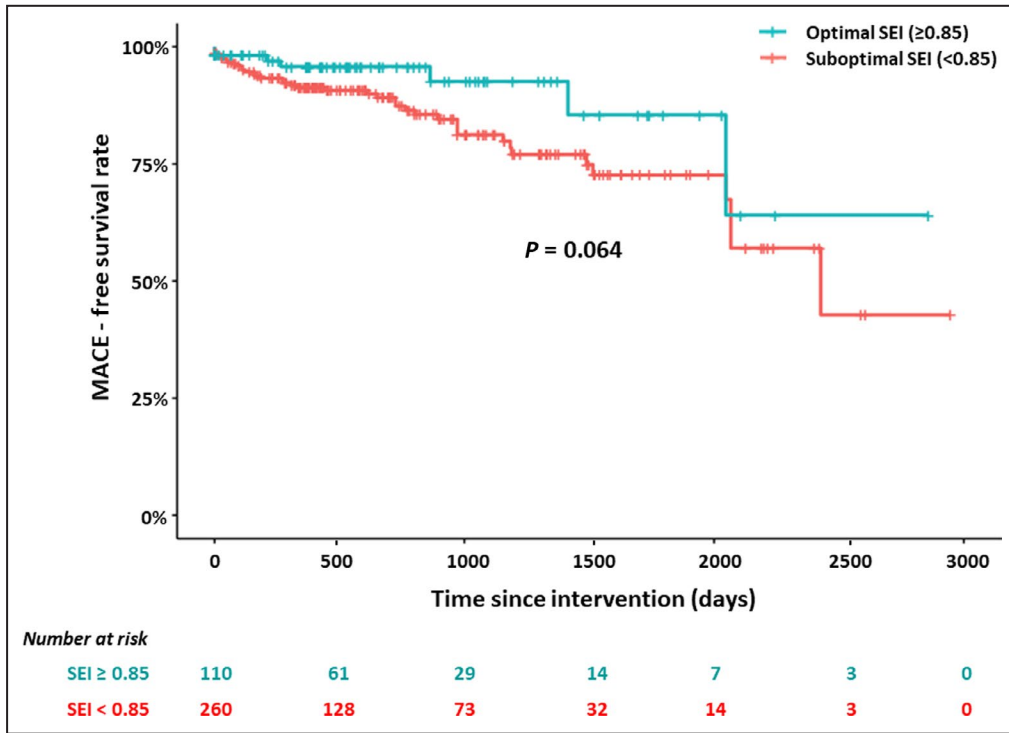


**Figure 4.** MACE-free survival rate between cases with optimal ( $\geq 0.85$ ) and suboptimal ( $< 0.85$ ) SEI.

MACE indicates major adverse cardiac events; and SEI, stent expansion index.

results of which are discussed in detail in Data S1. The Kaplan-Meier curve for MACE-free survival between lesions with optimal and suboptimal SEI also showed modest separation as in the complete cohort ( $P=0.066$ ) (Figure S2).

## DISCUSSION

In the current 370-lesion cohort, we aimed to define optimal stent expansion evaluated by OCT associated with lower incidence of MACE over time. In addition, we

**Table 4.** Qualitative Optical Coherence Tomography Characteristics

	Whole cohort (n=370)	Optimal SEI (n=110)	Suboptimal SEI (n=260)	P value
Thrombus	106 (28.6)	32 (29.1)	74 (28.5)	0.90
Plaque protrusion	113 (30.5)	31 (28.2)	82 (31.5)	0.54
Minor	113 (30.5)	31 (28.2)	82 (31.5)	
Major	0 (0)	0 (0)	0 (0)	
Untreated reference segment disease	66 (17.8)	17 (15.5)	49 (18.8)	0.46
Low lipid arc	31 (8.4)	8 (7.3)	23 (8.8)	
Medium lipid arc	25 (6.8)	8 (7.3)	17 (6.5)	
High lipid arc	10 (2.7)	1 (0.9)	9 (3.5)	
Dissection	55 (14.9)	13 (11.8)	42 (16.2)	0.34
Minor	43 (11.6)	12 (10.9)	31 (11.9)	
Major	12 (3.2)	1 (0.9)	11 (4.2)	
Malapposition	171 (46.2)	45 (40.9)	126 (48.5)	0.21
Minor	152 (41.1)	45 (40.9)	107 (41.2)	
Major	19 (5.1)	0 (0.0)	19 (7.3)	

Data shown as number (percentage); a P value of  $< 0.05$  was considered significant. Optimal stent expansion index (SEI) is defined as  $SEI \geq 0.85$ , whereas suboptimal SEI is defined as  $SEI < 0.85$ .



**Table 5. Morphometric Optical Coherence Tomography Analysis Results**

	Whole cohort (n=370)	Optimal SEI (n=110)	Suboptimal SEI (n=260)	P value
Visible stented length, mm	20.4 (15.2–27.0)	18.0 (14.3–23.6)	22.0 (15.8–28.0)	0.004
Lumen measurements				
Maximum lumen diameter, mm	3.54 (3.12–3.96)	3.55 (3.19–4.08)	3.53 (3.10–3.92)	0.23
Minimum lumen diameter, mm	2.83 (2.51–3.24)	3.05 (2.70–3.48)	2.77 (2.44–3.13)	<0.001
Mean lumen diameter, mm	3.16 (2.82–3.56)	3.27 (2.96–3.72)	3.11 (2.77–3.46)	0.001
Maximum lumen area, mm <sup>2</sup>	9.83 (7.67–12.32)	9.91 (7.98–13.08)	9.79 (7.56–12.05)	0.25
Minimum lumen area, mm <sup>2</sup>	6.29 (4.96–8.24)	7.30 (5.71–9.49)	6.01 (4.68–7.72)	<0.001
Mean lumen area, mm <sup>2</sup>	7.91 (6.27–10.00)	8.53 (6.88–10.92)	7.69 (6.06–9.47)	0.002
Stent measurements				
Maximum stent diameter, mm	3.39 (3.03–3.83)	3.52 (3.12–3.96)	3.34 (3.00–3.75)	0.02
Minimum stent diameter, mm	2.77 (2.44–3.18)	3.03 (2.68–3.44)	2.67 (2.34–3.09)	<0.001
Mean stent diameter, mm	3.10 (2.77–3.47)	3.23 (2.91–3.70)	3.03 (2.70–3.39)	<0.001
Maximum stent area, mm <sup>2</sup>	9.05 (7.22–11.54)	9.73 (7.63–12.32)	8.77 (7.09–11.05)	0.03
Minimum stent area, mm <sup>2</sup>	6.02 (4.66–7.92)	7.23 (5.64–9.31)	5.59 (4.30–7.48)	<0.001
Mean stent area, mm <sup>2</sup>	7.61 (6.02–9.46)	8.23 (6.67–10.76)	7.26 (5.79–9.08)	<0.001
Stent to lumen measurements				
Maximum stent to lumen area, mm <sup>2</sup>	0.19±0.47	0.34±0.44	0.13±0.47	<0.001
Minimum stent to lumen area, mm <sup>2</sup>	-1.23±1.00	-0.91±0.80	-1.37±1.05	<0.001
Mean stent to lumen area, mm <sup>2</sup>	-0.34±0.41	-0.17±0.29	-0.41±0.43	<0.001
Stent expansion index	0.79 (0.72–0.86)	0.91 (0.87–0.94)	0.74 (0.69–0.80)	<0.001

Data shown as median (interquartile range) or mean±SD; A P value of <0.05 was considered significant. Optimal stent expansion index (SEI) is defined as SEI ≥0.85, whereas suboptimal SEI is defined as SEI <0.85.

focused on reporting OCT-assessed stent expansion achieved in day-to-day practice among high-volume centers in a large proportion of patients undergoing PCI. In this regard, the most salient findings of the current study can be summarized as follows:

- (i) The median SEI was 0.79 (IQR, 0.72–0.86). Only 15.7% of lesions had an SEI of ≥0.9, while ≥0.8 and ≥0.7 was achieved in 45.1% and 78.4%, respectively.
- (ii) MACE incidence was 12.7% in our assessed cohort during a median of 557 (IQR, 323–1103) days post-PCI follow-up. OCT-derived SEI of <0.85 was associated with a higher incidence of MACE during post-PCI follow-up. Along with SEI <0.85, coronary calcification at baseline was found to be an independent predictor of MACE.

Stent underexpansion has been identified as a powerful predictor of worse post-PCI outcomes such as stent thrombosis<sup>10</sup> and angiographic restenosis.<sup>11</sup> OCT has the potential to significantly aid in assessing stent expansion because of its outperforming resolution in the near field permitting automated evaluation of SEI; a pragmatic measure of stent expansion relative to proximal and distal reference sites. In this regard, there is ongoing debate as to the most ideal cutoff of SEI, which is associated with a lower incidence of adverse cardiovascular events over time.

Variability in assessment of SEIs and its cutoffs is evident in published literature. The DOCTORS study<sup>1</sup> and European Association of Percutaneous Cardiovascular Interventions expert consensus document<sup>4</sup> suggest detection of just 1 MSA frame in the stented segment and dividing it with the average of proximal and distal lumen areas to obtain SEI. They also suggest such SEI of >80% to be optimal. On the other hand, the prospective ILLUMIEN III trial required splitting of stented segments into

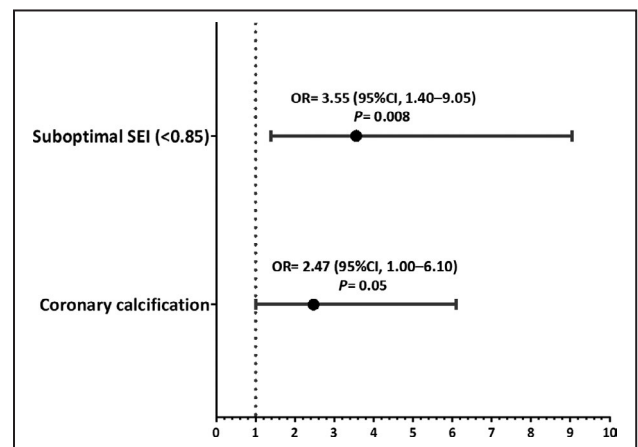


**Figure 5. Factors associated with post-percutaneous coronary intervention MACE.**

MACE indicates major adverse cardiac events; OR, odds ratio; and suboptimal SEI, lesions with stent expansion index <0.85.

2 halves and defined SEI cutoff of 90% in both halves to suggest optimal expansion.<sup>2</sup> In the subsequent ongoing ILUMIEN IV trial, the same strategy of stent optimization is advised. Without doubt, improved SEI as proposed in the ILUMIEN IV trial has theoretical advantage when compared with prior studies in this field; yet SEI achieved in daily practice remains largely unknown. Along these lines, we aimed to collect data on SEI from 5 large volume centers with great experience in using OCT to achieve optimal PCI results. In this regard, SEI of 90% in both halves was achieved in only 15.7% of our cases, which suggests it to be an ambitious target, at least in daily practice. Complex highly calcified lesions may be the rate-limiting factor in achieving higher expansion indices. Operators, while treating such lesions, may be reluctant to spend more time-consuming lesion preparation strategies such as debulking technologies, use of scoring/cutting balloons and super-high-pressure balloons, which incidentally are also associated with higher rates of procedural complications like atheroembolization, coronary dissection, and perforation. Unmodified focal calcium, and unresolved calcified nodules have been known to prevent optimal stent expansion. Trying to forcefully achieve  $\geq 90\%$  SEI in all cases has its own pitfalls. While modifying unconventional, thick, or deep calcified lesions, repeated pre- and postdilations may induce significant tissue injury, which may also promote restenosis and uncontrolled neointimal growth. Newer calcium modification modalities such as intravascular lithotripsy may be a potential game changer in this regard.<sup>12</sup> The Disrupt CAD III (Disrupt CAD III With the Shockwave Coronary IVL System) trial in its OCT subgroup demonstrated excellent results where shockwave lithotripsy induced longitudinal calcium fractures in 67.4% of OCT-imaged lesions, effecting an increase in post-PCI MSA.<sup>13</sup> The use of intravascular lithotripsy for stent optimization in tight, heavily calcified lesions therefore promises to be an exciting avenue.

To overcome limitations associated with predefined SEI goals to be achieved in daily practice, we aimed to establish such cutoff associated with increased incidence of MACE. In our cohort of 370 unselected lesions with available post-PCI OCT imaging, we were able to derive an SEI cutoff of  $< 0.85$  associated with unfavorable outcome. While this cutoff was associated with increased rates of MACE with high sensitivity over a median follow-up period of 557 days, its specificity remained rather low, at 0.34. Consequently, while achieving SEI  $< 0.85$  during the index PCI may practically be used to identify patients who are likely to suffer post-PCI MACE, the presence of SEI  $\geq 0.85$  alone may not permit us to correctly predict the risk of future MACE in this specific population. The latter fact is well explained by additional confounding variables that are associated with adverse cardiac events over time. In our analysis, moderate-severe calcification of coronary arteries was also found as an independent predictor of MACE over time, which partly explains the

lack of specificity of SEI in separating patients with future cardiovascular events. Most importantly, it must be acknowledged that the current analysis was mainly focused on revealing predictive metrics of stent expansion associated with future MACE. Consequently, the study may have been underpowered to consider well-known clinical factors of follow-up MACE in patients undergoing PCI. Future randomized trials are needed to consolidate these knowledge gaps.

The CLI-OPCI II (Centro per la Lotta contro l'Infarto–Optimisation of Percutaneous Coronary Intervention II) study adopted a similar retrospective approach to identify OCT-assessed predictors of significant follow-up events.<sup>14</sup> Presence of at least 1 significant OCT criteria among in-stent minimum lumen area  $< 4.5 \text{ mm}^2$ , distal/proximal dissection  $> 200 \mu\text{m}$ , in-stent lumen under-expansion ( $< 70\%$  of the mean reference lumen area), malapposition  $> 200 \mu\text{m}$ , intrastent plaque/thrombus protrusion, and distal/proximal reference lumen area  $< 4.5 \text{ mm}^2$  was found to be associated with follow-up MACE in the CLI-OPCI II study. In addition to substantial differences in clinical and procedural characteristics among the CLI-OPCI II and our population, several of our OCT parameters such as in-stent and reference lumen diameters and areas were larger (higher means) and possibly with greater variability (higher SDs), leading to a lower proportion of cases with minimum lumen area  $< 4.5 \text{ mm}^2$  as opposed to that in the CLI-OPCI cohort (18.1% vs. 23.4% respectively). While an absolute metric of minimum lumen area such as provided by CLI-OPCI II may hold significant advantage with regards to practicability in determining stent expansion in clinical practice, relative measures of stent expansion as applied in the current study may improve applicability to patient populations with broader inclusion criteria and vessel anatomy. Against this background, we found SEI to be significantly associated with MACE, which confirms the relevance of appropriate stent expansion to avoid adverse outcomes over time and extends the highly relevant findings of the CLI-OPCI II study to broader patient populations encompassing larger vessel size.

## Limitations

The present study is retrospective in nature and has several limitations. First, there is an issue of selection bias. A sizable number of lesions ( $n=242$ ; 39.5%) had to be excluded after initial quality check. There was low representation of complex lesions in our cohort. We see few lesions with (1) restenosis, (2) multiple overlapping stents, and (3) ST-segment–elevation MIs, all being major confounders of worse outcomes during follow-up. Second, there was little homogeneity in data collection of events during follow-up, where we see several outliers in follow-up durations. Also, event adjudication was retrospectively conducted by site investigators and not at a centralized facility, which is

not ideal. Third, our sample size (and follow-up duration) may be inappropriate to show significant differentiation of SEI subgroups with respect to MACE via Kaplan-Meier curves. Fourth, it is also noteworthy that our studied cohort lacks absolute homogeneity, as 17.6% of treated lesions received bioresorbable/resorbable scaffolds during the index PCI. Finally, SEI is only one of the many factors related to worse outcomes after PCI. Suboptimal lesion preparation and inappropriate stent sizing are also known to contribute substantially toward stent failure. The present study, however, did not focus on these.

## CONCLUSIONS

The present study identifies  $\geq 0.85$  as optimal SEI in daily practice. This cutoff also seems to be associated with lower incidence of future MACE during post-PCI follow-up. Along with SEI of  $< 0.85$ , coronary calcification also seems to be a significant predictor of post-PCI MACE. These results warrant further examination in larger, heterogeneous cohorts.

## ARTICLE INFORMATION

Received September 9, 2021; accepted March 4, 2022.

### Affiliations

Klinik für Herz- und Kreislauferkrankungen, Deutsches Herzzentrum München, Technische Universität München, Munich, Germany (H.R., F.H., M.S., A.A., E.X., S.K., S.C., A.K., M.J.); Cardiovascular Research Institute Dublin, Mater Private Network, Dublin, Ireland (H.R., R.A.B.); School of Pharmacy and Biomolecular Sciences, RCSI University of Medicine and Health Sciences, Dublin, Ireland (H.R., R.A.B.); Universitätsklinik für Kardiologie, Inselspital Bern, Bern, Switzerland (T.O., L.R.); Charité - Universitätsmedizin Berlin, Berlin, Germany (Y.S.A., D.M.L.); Hospital Universitario de La Princesa and Universidad Autónoma de Madrid, CIBERCV, Madrid, Spain (P.A., F.A.); Universitätsklinikum Gießen und Marburg, Giessen, Germany (F.B., H.N.); Klinikum rechts der Isar, Munich, Germany (T.K., K.-L.L.); ; DZHK (German Centre for Cardiovascular Research), partner site Berlin, Bern, Germany (Y.S.A., D.M.L.); and DZHK (German Centre for Cardiovascular Research), partner site Munich Heart Alliance, Munich, Germany (A.K., M.J.).

### Sources of Funding

None.

### Disclosures

Dr Leistner reports speaker as well advisory fees and research funding from Abbott Vascular. Dr Byrne reports research funding to the institution from Abbott Vascular, Biosensors, Biotronik, and Boston Scientific. Dr Joner reports personal fees from Biotronik, Orbus Neich, Recor, Astra Zeneca, Abbott, and Shockwave; grants and personal fees from Boston Scientific and Edwards; and grants from Amgen and Infraredx, outside the submitted work. The remaining authors have no disclosures to report.

### Supplemental Material

Data S1  
Table S1  
Figures S1–S2

## REFERENCES

- Meneveau N, Souteyrand G, Motreff P, Caussin C, Amabile N, Ohlmann P, Morel O, Lefrançois Y, Descotes-Genon V, Silvain J, et al. Optical coherence tomography to optimize results of percutaneous coronary intervention in patients with non-ST-elevation acute coronary syndrome: results of the multicenter, randomized DOCTORS study (Does Optical Coherence Tomography Optimize Results of Stenting). *Circulation*. 2016;134:906–917. doi: 10.1161/CIRCULATIONAHA.116.024393
- Ali ZA, Maehara A, Généreux P, Shlofmitz RA, Fabbiochi F, Nazif TM, Guagliumi G, Meraj PM, Alfonso F, Samady H, et al. Optical coherence tomography compared with intravascular ultrasound and with angiography to guide coronary stent implantation (ILUMIEN III: OPTIMIZE PCI): a randomised controlled trial. *Lancet*. 2016;388:2618–2628. doi: 10.1016/S0140-6736(16)31922-5
- Buccheri S, Franchina G, Romano S, Puglisi S, Venuti G, D'Arrigo P, Francaviglia B, Scalia M, Condorelli A, Barbanti M, et al. Clinical outcomes following intravascular imaging-guided versus coronary angiography-guided percutaneous coronary intervention with stent implantation: a systematic review and Bayesian network meta-analysis of 31 studies and 17,882 patients. *JACC Cardiovasc Interv*. 2017;10:2488–2498. doi: 10.1016/j.jcin.2017.08.051
- Räber L, Mintz GS, Koskinas KC, Johnson TW, Holm NR, Onuma Y, Radu MD, Joner M, Yu BO, Jia H, et al. Clinical use of intracoronary imaging. Part 1: guidance and optimization of coronary interventions. An expert consensus document of the European Association of Percutaneous Cardiovascular Interventions. *EuroIntervention*. 2018;14:656–677. doi: 10.4244/EIJY18M06\_01
- Ryan TJ, Faxon DP, Gunnar RM, Kennedy JW, King SB 3rd, Loop FD, Peterson KL, Reeves TJ, Williams DO, Winters WL Jr, et al. Guidelines for percutaneous transluminal coronary angioplasty. A report of the American College of Cardiology/American Heart Association Task Force on Assessment of Diagnostic and Therapeutic Cardiovascular Procedures (Subcommittee on Percutaneous Transluminal Coronary Angioplasty). *Circulation*. 1988;78:486–502. doi: 10.1161/01.cir.78.2.486
- Mintz GS, Popma JJ, Pichard AD, Kent KM, Satler LF, Chuang YC, Ditrano CJ, Leon MB. Patterns of calcification in coronary artery disease. A statistical analysis of intravascular ultrasound and coronary angiography in 1155 lesions. *Circulation*. 1995;91:1959–1965. doi: 10.1161/01.cir.91.7.1959
- Thygesen K, Alpert JS, Jaffe AS, Simoons ML, Chaitman BR, White HD; Writing Group on the Joint ESCAAHAWHFTffUDOMI, Thygesen K, Alpert JS, White HD, et al. Third universal definition of myocardial infarction. *Eur Heart J*. 2012;33:2551–2567. doi: 10.1093/eurheartj/ehs184
- Cutlip DE, Nakazawa G, Krucoff MW, Vorpahl M, Mehran R, Finn AV, Vranckx P, Kimmelstiel C, Berger C, Petersen JL, et al. Autopsy validation study of the academic research consortium stent thrombosis definition. *JACC Cardiovasc Interv*. 2011;4:554–559. doi: 10.1016/j.jcin.2011.01.011
- Cutlip DE, Windecker S, Mehran R, Boam A, Cohen DJ, van Es G-A, Gabriel Steg P, Morel M-A, Mauri L, Vranckx P, et al. Clinical end points in coronary stent trials: a case for standardized definitions. *Circulation*. 2007;2344–2351. doi: 10.1161/CIRCULATIONAHA.106.685313
- Fujii K, Carlier SG, Mintz GS, Yang Y-M, Moussa I, Weisz G, Dangas G, Mehran R, Lansky AJ, Kreps EM, et al. Stent underexpansion and residual reference segment stenosis are related to stent thrombosis after sirolimus-eluting stent implantation: an intravascular ultrasound study. *J Am Coll Cardiol*. 2005;45:995–998. doi: 10.1016/j.jacc.2004.12.066
- Hong MK, Mintz GS, Lee CW, Park DW, Choi BR, Park KH, Kim YH, Cheong SS, Song JK, Kim JJ, et al. Intravascular ultrasound predictors of angiographic restenosis after sirolimus-eluting stent implantation. *Eur Heart J*. 2006;27:1305–1310. doi: 10.1093/eurheartj/ehi882
- Ali ZA, Nef H, Escaned J, Werner N, Banning AP, Hill JM, De Bruyne B, Montorfano M, Lefevre T, Stone GW, et al. Safety and effectiveness of coronary intravascular lithotripsy for treatment of severely calcified coronary stenoses: the Disrupt CAD II study. *Circ Cardiovasc Interv*. 2019;12:e008434. doi: 10.1161/CIRCINTERVENTIONS.119.008434
- Hill JM, Kereiakes DJ, Shlofmitz RA, Klein AJ, Riley RF, Price MJ, Herrmann HC, Bachinsky W, Waksman R, Stone GW, et al. Intravascular lithotripsy for treatment of severely calcified coronary artery disease. *J Am Coll Cardiol*. 2020;76:2635–2646. doi: 10.1016/j.jacc.2020.09.603
- Prati F, Romagnoli E, Burzotta F, Limbruno U, Gatto L, La Manna A, Versaci F, Marco V, Di Vito L, Imola F, et al. Clinical impact of OCT findings during PCI: the CLI-OPCI II study. *JACC Cardiovasc Imaging*. 2015;8:1297–1305. doi: 10.1016/j.jcmg.2015.08.013

# **Supplemental Material**

## **Data S1.**

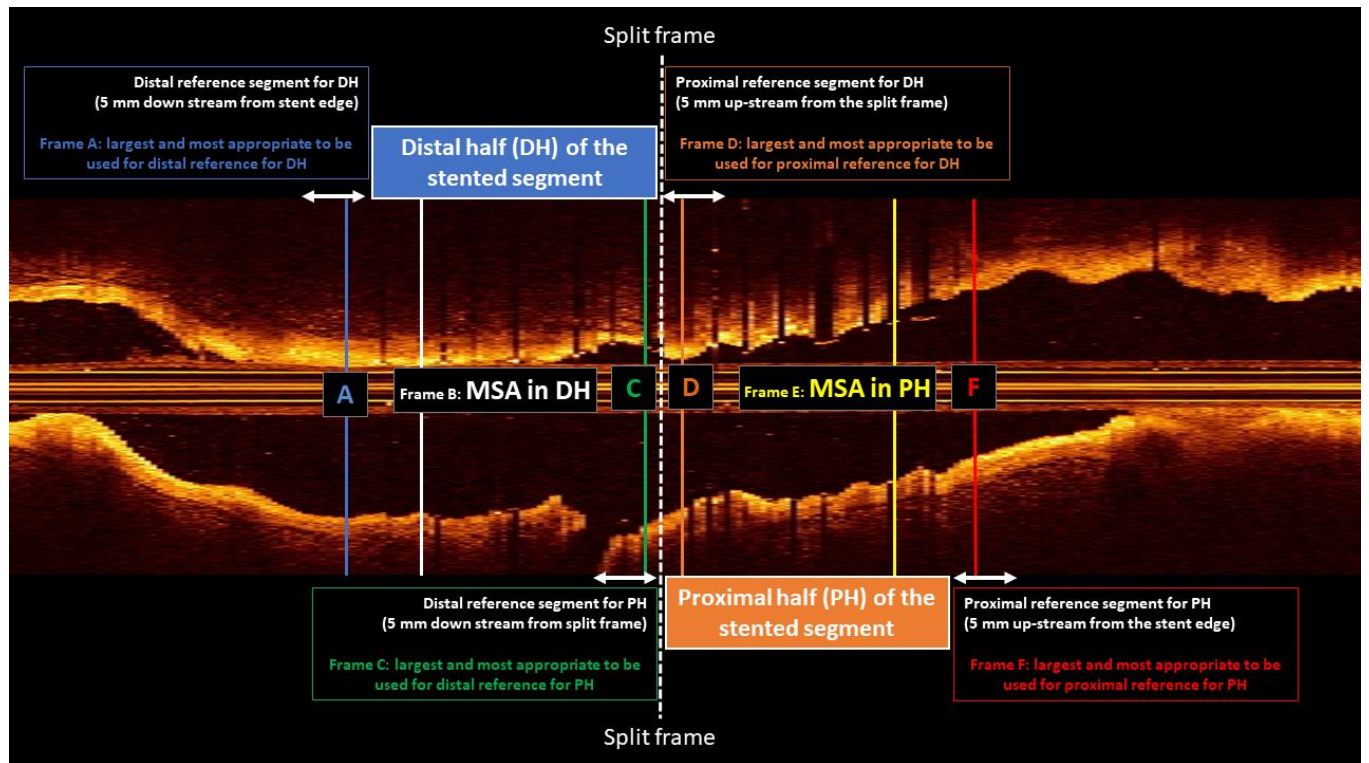
### **Reference frame selection**

In majority of cases (without large side branches) the split occurred from the middle of the stented segment. The optical coherence tomography (OCT) frame with the largest lumen area downstream within 5-mm of split frame became the distal reference frame of the proximal half of the stented segment (Frame C in the **Figure S1**). On the other hand, the frame with the largest lumen area upstream within 5-mm of the split frame became the proximal reference frame for the distal half of the stented segment (Frame D in the **Figure S1**). In cases with a large side branch opening of  $\geq 2.5$ mm contained within the stented segment, the split occurred at the mid-point of the bifurcation. In such cases the stent area at the split frame was considered as the proximal reference lumen area of the distal half of the stented segment as well as the distal reference lumen area for the proximal half of the stented segment.

Similar process was followed for the edge segments (i) frame with the largest lumen area 5-mm downstream from the distal stent edge was considered as the distal reference area for the distal half of the stented segment (Frame A in the **Figure S1**), (ii) frame with the largest lumen area 5-mm upstream from the proximal stent edge was considered as the proximal reference area for the proximal half of the stented segment (Frame F in the **Figure S1**).

Reference frame selection process was modified when either of the stent edges landed near a opening of large side branch. In such case the representative lumen area within the stented segment nearest to the concerned stent edge was taken a reference.

**Figure S1. Reference frame selection process for stented segments split from the middle**



DH, distal half, PH, proximal half, MSA, minimum stent area

### Qualitative OCT assessment

Qualitative OCT assessment of analyzed lesions are summarized in **Table 4**. Overall, 28.6% lesions had visible of thrombus within the stented segment. Cases with visible thrombus were numerically higher in the optimal SEI subgroup as compared to the sub-optimal SEI subgroup (29.1 vs. 28.5%,  $p=0.90$ ). Overall, plaque protrusion was present in 30.5% of cases and numerically lower within optimal SEI subgroup as compared to the sub-optimal SEI subgroup (28.2 vs. 31.5%,  $p=0.54$ ). There were no cases with major plaque protrusion in our sample. Untreated reference segment disease was present in 17.8% of cases in the whole cohort and

numerically higher in sub-optimal SEI subgroup than in optimal SEI subgroup (18.8 vs. 15.5%,  $p= 0.46$ ). Untreated segment disease with high lipid arcs was also more prevalent in the sub-optimal SEI subgroup (3.5 vs. 0.9%). Dissection was present in 14.9% of the whole cohort, amongst which 11.6% were minor. Dissections were also numerically higher in the sub-optimal SEI subgroup as compared to the optimal SEI subgroup (16.2 vs. 11.8%,  $p= 0.34$ ). Overall, 46.2% lesions had one or more malapposed struts, in which 5.1% were classified as major malapposition. All malapposition (48.5 vs. 40.9%,  $p= 0.21$ ) and major malapposition (7.3 vs. 0%) were also numerically higher in the sub-optimal SEI subgroup as compared to the optimal SEI subgroup.

### **Morphometric OCT analysis**

Results of morphometric OCT analysis are summarized in **Table 5**. Visible/analyzable stented length in the whole cohort was 20.4 (15.2, 27.0) mm. Visible stented length was significantly higher in the sub-optimal SEI subgroup as compared to the optimal SEI subgroup [22.0 (15.8, 28.0) vs. 18.0 (14.3, 23.6) mm,  $p= 0.004$ ]. Maximum, minimum, and mean lumen diameters in the whole cohort were 3.54 (3.12, 3.96), 2.83 (2.51, 3.24) and 3.16 (2.82, 3.56) mm respectively, while maximum, minimum and mean lumen areas were 9.83 (7.67, 12.32), 6.29 (4.96, 8.24) and 7.91 (6.27, 10.0) mm<sup>2</sup> respectively. Minimum and mean lumen diameters ( $p<0.001$  and 0.001 respectively) and areas ( $p<0.001$  and 0.002 respectively) were significantly higher in optimal SEI subgroup as compared to sub-optimal SEI subgroup. Maximum lumen diameters and areas were however comparable between the two subgroups ( $p= 0.23$  and 0.25 respectively).

Amongst stent measurements in the whole cohort, maximum, minimum and mean diameters were 3.39 (3.03, 3.83), 2.77 (2.44, 3.18) and 3.10 (2.77, 3.47) mm respectively, while maximum, minimum and mean areas were 9.05 (7.22, 11.54), 6.02 (4.66, 7.92) and 7.61 (6.02, 9.46) mm<sup>2</sup> respectively. Minimum and mean stent diameters (p<0.001 for both) and areas (p<0.001 for both) were significantly higher in optimal SEI subgroup as compared to sub-optimal SEI subgroup. Maximum stent diameters and areas similarly were also significantly higher in the optimal SEI subgroup as compared to the sub-optimal SEI subgroup (p= 0.02 and 0.03 respectively).

Overall, maximum stent to lumen area was 0.19±0.47 mm<sup>2</sup>, minimum stent to lumen area was -1.23±1.00 mm<sup>2</sup>, while mean stent to lumen area was -0.34±0.41 mm<sup>2</sup>. Maximum stent to lumen area was significantly higher in the optimal SEI subgroup (0.34±0.44 vs. 0.13±0.47 mm<sup>2</sup>, p<0.001), however minimum and mean stent to lumen areas were lower in the optimal SEI subgroup as compared to the sub-optimal SEI subgroup (-0.91±0.80 vs. -1.37±1.05 mm<sup>2</sup>, p<0.001 and -0.17±0.29 vs -0.41±0.43 mm<sup>2</sup>, p<0.001 respectively).

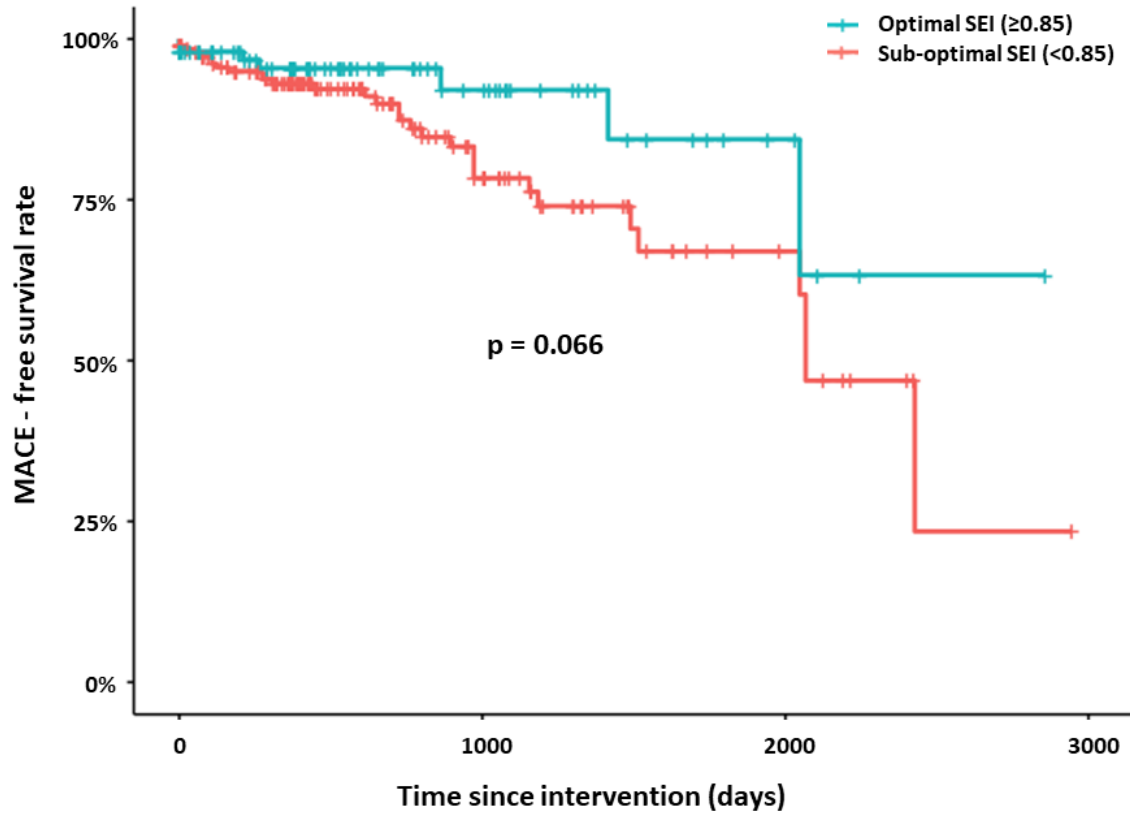
SEI (minimum) in the whole cohort was 0.79 (0.72, 0.86), while significantly higher in the optimal SEI subgroup as compared to the sub-optimal SEI subgroup [0.91 (0.87, 0.94) vs. 0.74 (0.69, 0.80), p<0.001]. SEI of ≥0.90 was achieved in 15.7%, ≥0.80 in 45.1% and ≥0.70 in 78.4% cases. Inter and intra-rater reliability was tested for SEI and was found to be excellent in 20 randomly selected reanalyzed lesions (ICC= 0.85 and 0.89 respectively).



## **Sensitivity analysis**

Sensitivity analysis was performed where we excluded lesions treated with bioresorbable vascular scaffold or resorbable magnesium scaffolds (excluded n= 65, 17.6% lesions; analyzed 305 lesions). Generalized regression analysis identified triple vessel disease (0.0324), coronary calcification (p= 0.0156) and suboptimal SEI (p= 0.0059) as predictors of follow-up MACE. Subsequent adaptive LASSO regression, however, was not able to identify any independent factors capable of predicting MACE during follow-up. Kaplan-meier curve for MACE free survival was generated amongst optimal SEI ( $SEI \geq 0.85$ , n= 104) and sub-optimal SEI ( $SEI < 0.85$ , n= 201) subgroups. As in the complete cohort the curves showed modest separation between the subgroups; however, the difference did not reach statistical significance (p= 0.066) (**Figure S2**).

Figure S2. MACE -free survival rate between cases with optimal ( $\geq 0.85$ ) and sub-optimal ( $< 0.85$ ) SEI in our sensitivity cohort.



MACE, major adverse cardiac events; SEI, stent expansion index

**Table S1. Medications prescribed at hospital discharge.**

<i>Lesions</i>	<i>370</i>
Aspirin*	349 (94.6)
Adenosine diphosphate (ADP) receptor antagonists	370 (100)
Oral anticoagulation*	46 (12.5)
Beta-blockers*	280 (75.9)
Angiotensin-converting enzyme inhibitors /	317 (85.9)
Angiotensin II receptor blockers*	
Statins	353 (95.4)

Data expressed here is lesion based and shown as number (percentage); \* data available for 99.7% of study sample (369 lesions).